

# Organic FET devices based upon latent pigments of unsubstituted diketopyrrolopyrrole or quinacridone

Hiroyuki Yanagisawa, Jin Mizuguchi; Graduate School of Engineering, Yokohama National University; 79-5 Tokiwadai, Hodogaya-ku, 240-8501 Yokohama, Japan; Shinji Aramaki and Yoshimasa Sakai; Mitsubishi Chemical Group Science & Technology Research Center; 1000 kamoshida-cho, aoba-ku, Yokohama, Japan

## Abstract

Organic FETs based upon unsubstituted diketopyrrolopyrrole (DPP) or quinacridone (QA) have been fabricated, using their solvent-soluble precursors called latent pigments (*t*-BOC DPP and *t*-BOC QA) that can be also regenerated into their parent pigments by heating around 200 °C. Use of latent pigments enables us to fabricate FET devices by means of spin coating, offering a low-cost fabrication process rather than an expensive vacuum technology. The objective of the present investigation is to evaluate the performance of DPP- and QA-based FETs prepared by latent pigments. As a result, the field effect mobilities of about  $7.19 \times 10^{-6}$  and  $8.23 \times 10^{-6}$  cm<sup>2</sup>/Vs have been obtained for FET devices based upon *t*-BOC DPP and QA, respectively. These values are almost equivalent to those of the FETs prepared by vacuum deposition of DPP and QA:  $1.43 \times 10^{-5}$  and  $1.08 \times 10^{-5}$  cm<sup>2</sup>/Vs, respectively. The present result leads us to conclude that the latent pigment technology is a promising low-cost process to fabricate organic FETs.

## 1. Introduction

Recently, a number of field effect transistor (FET) have been fabricated with thin films of organic materials. The field effect mobility of the organic FETs is still much lower than those of inorganic FETs. However, the organic FETs have certain advantages in low fabrication costs and large area device fabrication that is carried out at room temperature. Their target is therefore toward flexible display and IC tag applications, and the solution-processibility is one of the key issues in order to achieve low-coat FETs by means of spin coating.

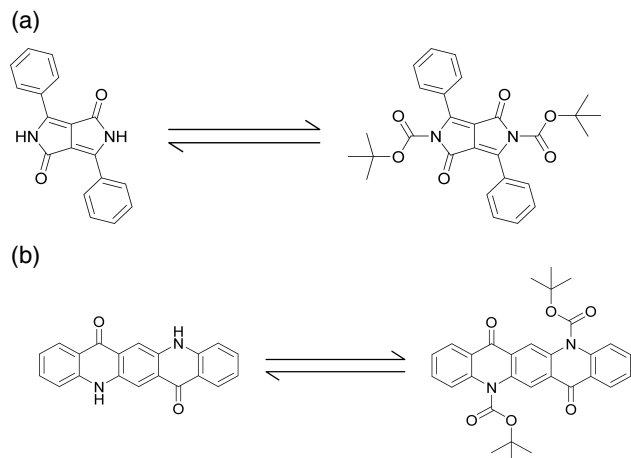
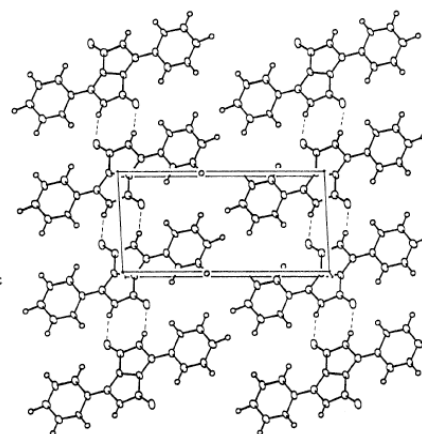


Fig. 1 Molecular structure: (a) DPP and *t*-BOC DPP, (b) QA and *t*-BOC QA.

We have previously reported that the metal-free porphyrin, so-called benzoporphyrin (BP), exhibits an excellent FET characteristic.<sup>1)</sup> Our FET system is characterized by use of a solvent-soluble BP-precursor and its thermal transformation into BP directly on the substrate at about 200 °C. Quite recently, we have also reported that copper-integrated BP (CuBP) shows an even better FET performance as characterized by a high mobility of about 1.3 cm<sup>2</sup>/Vs.<sup>2)</sup>

(a)



(b)

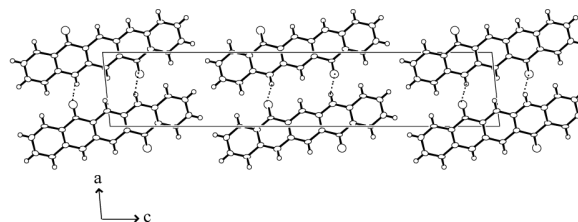


Fig. 2 Molecular arrangement: (a) DPP and (b)  $\beta$ -QA.

In this study, we will present another type of solvent-soluble precursors called latent pigment<sup>3-5)</sup> for fabricating organic FETs through solution process. We deal here with two kinds of latent pigments based upon diketopyrrolopyrrole (DPP: Fig. 1(a)) and quinacridone (QA: Fig. 1(b)) that are typical of the hydrogen-bonded pigments: *t*-BOC DPP and *t*-BOC QA. DPP and QA are industrially important red colorants which belong to the class of hydrogen-bonded pigments.<sup>6)</sup> In the solid state, there are chains of NH...O intermolecular hydrogen bonds between the NH group of one molecule and the O atom of the neighboring one, as shown in

Figs. 2(a)<sup>7</sup> and 2(b)<sup>8</sup>. The NH...O hydrogen bonds have two important functions.<sup>9</sup> One is to align the transition dipole in a fashion "head to tail" to displace the absorption band toward longer wavelengths on going from solution to the solid state. The other is to bridge small molecules of pigments together to impart a polymer-like stability.

The "latent pigment" has been developed by Zambounis, Hao and Iqbal at CIBA Specialty Chemicals.<sup>3,4</sup> The soluble precursor is prepared by replacing the H atom of the NH group with a *t*-butoxycarbonyl (*t*-BOC) group. The insoluble parent pigment can then be regenerated by thermal treatment of the precursor around 180-200 °C. The regeneration process of *t*-BOC DPP<sup>10</sup> and QA<sup>11</sup> as well as their crystal structures<sup>12-14</sup> have extensively been studied.

Our goal is to fabricate organic FETs based upon latent pigments of DPP or QA, and compare their performance with that of vacuum-deposited FETs of commercial DPP and QA.

## 2. Experimental

### 2-1. Preparation of latent pigments

*t*-BOC DPP and QA were prepared using DPP or QA (both of which are from Ciba Specialty Chem.) according to the methods previously reported.<sup>3,4</sup> Both *t*-BOC products were yellowish powders.

### 2-2. Fabrication of the FET devices

Two kinds of FET devices have been fabricated: spin-coated FET with latent pigments and vacuum-evaporated FET with commercial pigments.

The FET structure is depicted as shown in Fig. 3. A SiO<sub>2</sub>-layer of about 300 nm was thermally grown on a heavily doped *n*-type Si-substrate which serves as the gate electrode. On top of SiO<sub>2</sub>, the source and drain electrodes made of Au (1000 Å)/Cr (50 Å) were prepared by photolithographic technology. The channel length and the channel width were 10 and 500 μm, respectively.

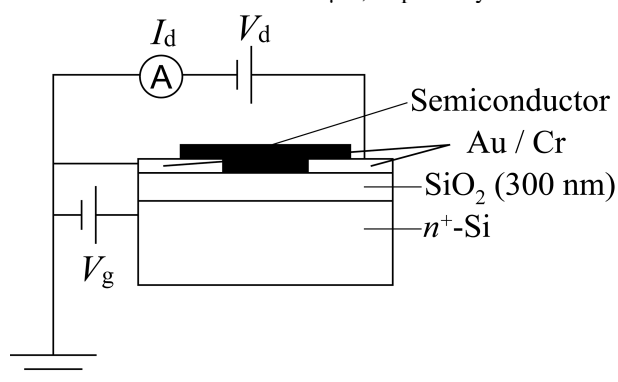


Fig. 3 Structure of the FET

Spin-coating was carried out on the channel of FET substrates using chloroform solution of *t*-BOC DPP (8.7 wt%) or *t*-BOC QA (8.7 wt%) at a rate of 1000 rpm for 30 s. Then, the film was converted into DPP or QA by heating at 220 °C for 15 min.

Vacuum-deposited films were prepared in the following way. Commercial DPP and β-QA were purified three times by sublimation under vacuum, and then evaporated onto the channel of FET substrates. The thickness of evaporated films is about 1000 Å.

## 2-3. Equipment

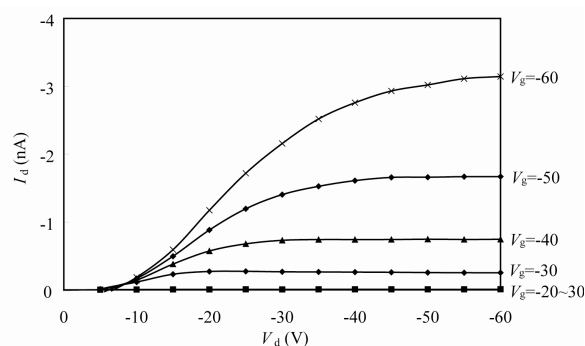
The *I*-*V* characteristics of the FETs were measured under vacuum with an Agilent 4155C semiconductor parameter analyzer. Scanning electron microscopy (SEM) photographs were made by VE-8800 REAL 3D system from KEYENCE. Powder X-ray diffraction diagrams were measured on a Rigaku diffractometer (model: Rapid F). X-ray diffraction diagrams of thin films were measured on a Rigaku RINT2000.

## 3. Results and Discussion

### 3-1. FET characteristics

The field effect mobility ( $\mu$ ) and threshold voltage ( $V_t$ ) were deduced from the  $I_{sat}^{1/2}$ - $V_g$  plot on the basis of the equation:  $I_{sat} = ((C_i W)/(2 L)) \mu V_g - V_t^2$ , where  $I_{sat}$ ,  $C_i$ ,  $W$ , and  $L$  stand for the saturation current, the capacitance of the insulator layer per unit area, the channel width and the channel length, respectively. The "on/off" ratio is defined as the ratio of drain current at  $V_g = -50$  V to that at  $V_g = 30$  V while the drain voltage is kept constant at  $V_d = -30$  V.

(a)



(b)

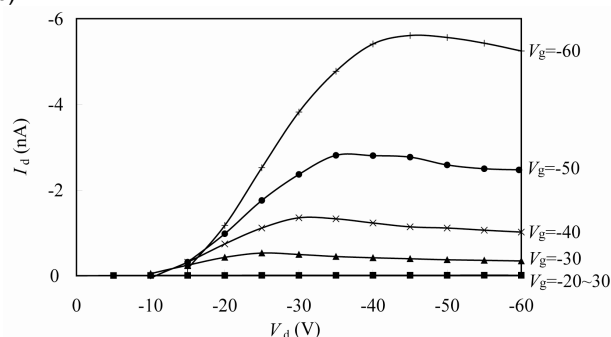
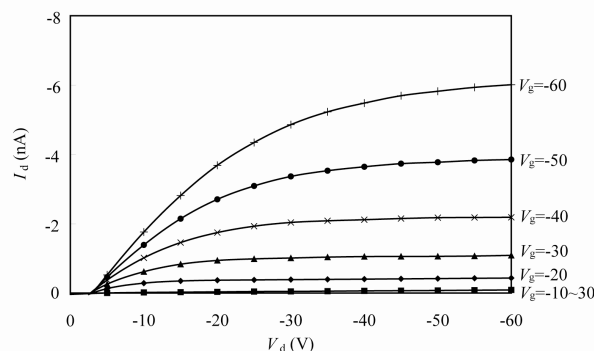


Fig. 4 *I*-*V* Characteristics: (a) spin-coated FET based upon DPP, (b) vacuum-deposited FET based upon commercial DPP

Figs. 4 (a) and 4(b) show the "drain current"- "drain voltage" ( $I_d$ - $V_d$ ) plot measured at room temperature under vacuum for spin-coated and vacuum-deposited FETs based upon DPP, respectively. The curves are typical of the FET characteristics and composed of a linear region at low  $V_d$  and a saturation region at high  $V_d$ . The negative sign of the drain and gate voltages indicates a hole transport of DPP. The field effect mobilities are  $7.19 \times 10^{-6}$  and  $1.43 \times 10^{-5}$  cm<sup>2</sup>/Vs, respectively, and the "on/off" ratios are 105 and 326 for spin-coated and vacuum-deposited FETs. It is remarkable to note that the mobility and the "on/off" ratio of spin-coated FETs are as large as those of vacuum-deposited FETs.

Likewise, Figs. 5 (a) and 5(b) show the “drain current”-“drain voltage” ( $I_d$ - $V_d$ ) plot for spin-coated and vacuum-deposited FETs based upon QA, respectively. The field effect mobilities are  $8.23 \times 10^{-6}$  and  $1.08 \times 10^{-5}$   $\text{cm}^2/\text{Vs}$ , respectively, and the “on/off” ratios 39 and 45. Here again, the hole transport is confirmed. In addition, no significant difference in FET performance is observed between spin-coated and vacuum-deposited FETs.

(a)



(b)

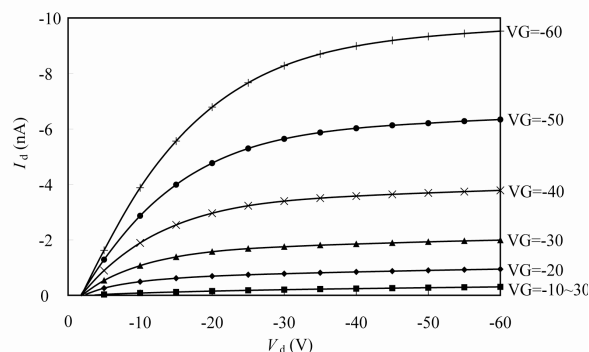


**Fig. 5**  $I$ - $V$  Characteristics: (a) spin-coated FET based upon QA, (b) vacuum-deposited FET based upon  $\beta$ -QA

### 3-2. Crystalline state of DPP and QA films

Fig. 6 shows the X-ray diffraction diagrams of powdered DPP, “spin-coated/regenerated” film and vacuum-deposited film on glass substrate. The diffraction peaks are assigned as shown on the basis of the crystallographic data of single crystals.<sup>12, 13)</sup> The diffraction peak around  $2\theta = 27^\circ$  ((1-11)) correspond to the diffractions along the stacking axis of the molecules. In all samples, the diffraction peaks of (001), (012) and (1-11) appear in common and no significance difference is recognized between these three diagrams. Furthermore, the molecules are not oriented in a particular direction with respect to the substrate, but are oriented in all directions just in the case of powders (diagram (a)).

However, the situation is different in  $\beta$ -QA. Fig. 7 shows the X-ray diffraction diagrams of powdered  $\beta$ -QA, “spin-coated/regenerated” film and vacuum-deposited film on glass substrate. The diffraction peaks are assigned as shown on the basis of the crystallographic data of single crystal.<sup>14)</sup> In “spin-coated/regenerated” film, one small diffraction appears at  $2\theta = 7^\circ$  which corresponds to the (002) plane, but no diffraction around  $27^\circ$ .

The indicates that the molecules are arranged along the  $c$ -axis perpendicular to the substrate (see Fig. 2(b) and that the molecules are not ordered along the stacking  $b$ -axis. On the other hand, in vacuum-deposited films, there observed only one diffraction peak around  $27^\circ$  ((1-11)) which corresponds to the diffraction along the stacking axis. This means that the molecules are stacked along the stacking  $b$ -axis in parallel to the substrate. However, it is important to note that the present molecular orientation is not reflected in the FET performance between these two samples. That is, no correlation between the crystalline state and the FET characteristics is available in FETs based upon QA.

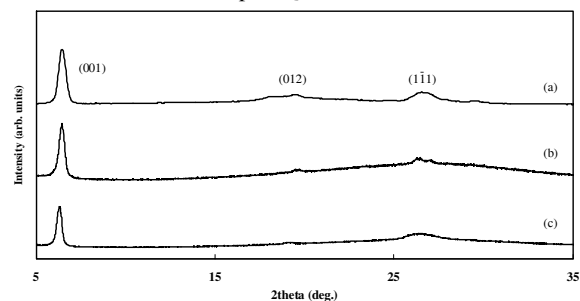


**Fig. 6** X-ray diffraction diagrams: (a) powder of DPP, (b) “spin-coated/regenerated” film of DPP on glass, and (c) evaporated film of commercial DPP on glass.

## 4. Conclusions

DPP- and QA-based FETs have been investigated on the basis of the latent pigment technology with special attention to the low-cost fabrication process. The FET devices fabricated by  $t$ -BOC DPP and  $t$ -BOC QA are found to exhibit nearly equivalent FET characteristics to those of vacuum-deposited FET prepared by evaporating commercial DPP and QA. This suggests that the  $t$ -BOC latent-pigment technology provides us with a new low-cost fabrication process of FETs.

## References

- 1) S. Aramaki, Y. Sakai and N. Ono: Solution-processible organic semiconductor for transistor applications: Tetrabenzo-porphyrin, Appl. Phys. Lett., **84**, 2085-2087 (2005).
- 2) S. Aramaki, A. Ohno, Y. Sakai and R. Yoshiyama: Field Effect Transistor, (2006). Jpn. Pat. 2006-165533 A 2006.6.22. pp. 1-28.
- 3) J. Zambounis, Z. Hao and A. Iqbal, Latent pigments activated by heat, A. Nature, **388**, 131 (1997).
- 4) J. Zambounis, Z. Hao and A. Iqbal. Pyrrolo[3,4- $c$ ]pyrroles, US Patent 5 484 943.
- 5) J. Mizuguchi: Latent pigments —Latent pigment technologies in hydrogen bonded pigments and their regeneration process—, J. Imag. Soc. Jpn, **44**, 347-355 (2005).
- 6) W. Herbst and K. Hunger: Industrial Organic Pigments **1993**, VCH, Weinheim, 550-553.
- 7) J. Mizuguchi, A. Grubenmann, G. Wooden and G. Rihs: Structure of 3,6-diphenylpyrrolo[3,4- $c$ ]pyrrole-1,4-dione and 3,6-diphenyl-2,5-dimethylpyrrolo [3,4- $c$ ] pyrrole-1,4-dione, Acta Cryst. B **48**, 696-700 (1992).
- 8) N. Nishimura, T. Senju and Mizuguchi: 5,7,12,14-Tetrahydro[2,3- $b$ ]quinolinoacridine ( $\beta$ form), Acta Cryst., **E62**, o4683-o4685 (2006).
- 9) J. Mizuguchi: Correlation between crystal and electronic structures in

- diketopyrrolopyrrole pigments as viewed from exciton coupling effects, J. Phys. Chem. A., **104**, 1817-1821 (2000).
- 10) J. Mizuguchi: A Pigment Precursor Based on 1,4-keto-3,6-diphenylpyrrolo-[3,4-*c*]-pyrrole and its Regeneration into the Pigment, J. Imag. Sci. Tech **49**, 35-40 (2005).
  - 11) Y. Imura, Y. Yamashita, T. Senju and J. Mizuguchi: Crystal Structure of a quinacridone pigment-precursor and its regeneration process, J. Imag. Soc. Jpn., **155**, 138-142 (2005).
  - 12) J. Mizuguchi, Refinement of the crystal structure of  $\alpha$ -1,4-dioxo- 3,6-diphenylpyrrolo-[3,4-*c*]pyrrole-2,5(1*H*,4*H*)-dicarboxylic acid bis (1,1-dimethylethyl) ester, Z. Krist. NCS. **218**, 134-136 (2003).
  - 13) J. Mizuguchi: The  $\beta$ -form of di-*tert*-butyl-1,4-dioxo-3,6-diphenyl-1,2,4,5-tetrahydropyrrolo[3,4-*c*]pyrrole-2,5-dicarboxylate, Acta Cryst. **E59**, o469-o471 (2003).
  - 14) J. Mizuguchi: Di-*tert*-butyl-7,14-dihydro-7,14-dioxoquino[2,3-*b*]acridine-5,12-dicarboxylate, Acta Cryst. **E 59**, o474-o475 (2003).

## Author Biography

*Hiroyuki Yanagisawa received his Bachelor of Engineering in 2005 and his Master of Engineering in 2007, both from Yokohama National University. Currently, he is working at Sony Corporation. His research interest includes structure analysis of organic pigments and their electronic applications. E-mail: Mizu-j@ynu.ac.jp*